Journal of Physics: Conference Series **398** (2012) 012012 doi:10.1088/1742-6596/398/1/012012

Influence of the shielding currents lengthscale and anisotropy effects on the magnetic flux profiles of high-temperature superconductors

P Vanderbemden[1] and V Lovchinov[2]

[1] University of Liège, SUPRATECS research group, Department of Electrical Engineering & Computer science (B28), Sart-Tilman, B-4000 Liège, Belgium
[2] Institute of Solid State Physics, Bulgarian Academy of Sciences, 72 Tzarigradsko Chaussee Blvd., 1784 Sofia, Bulgaria

E-mail : Philippe.Vanderbemden@ulg.ac.be

Abstract. The so-called "magnetic flux profile" AC inductive technique is a powerful method for determining the critical current density J_c of bulk superconductors. In this work we aim at reporting analytical expressions for magnetic flux profiles of superconducting rectangular samples exhibiting a critical current density anisotropy. The results are used for examining the error resulting from approximating a rectangular cross-section by an "infinite cylinder" or "infinite slab" geometry. It is found that such approximations can lead to an artificial curvature of the flux profiles and errors of 10%-20% in the determination of J_c. Next, the effects of how planar defects (cracks, platelet boundaries,...) affect the magnetic flux profile signal are discussed. It is found that the magnetic flux profiles are much sensitive to the lengthscale of shielding currents, thereby providing means of investigation of the typical size of induced current loops in bulk superconductors. Finally some illustrative flux profile data measured on a bulk, large grain melt-processed YBCO single domain exhibiting J_c anisotropy are presented and discussed in relation with theoretical predictions.

1. Introduction

Thanks to their zero electrical resistance at cryogenic temperature, superconducting materials represent a promising way of designing attractive electrical engineering applications [1-3]. In particular, when $YBa_2Cu_3O_{7-\delta}$ (YBCO) superconductors are cooled at the liquid nitrogen temperature (T = 77 K), they can carry current densities larger than 10 kA/cm² [4-5] and trap magnetic flux densities in excess of 2 teslas. The key physical parameter determining the practical usefulness of superconductors is the maximum current density that can flow without dissipation, i.e. the critical current density J_c. Due the usually high values of J_c, the reliable and accurate determination of the critical current density is sometimes a challenge. Basically, either *transport* methods or *magnetic* methods can be used. In transport measurements, the current is directly injected through the specimen. Magnetic measurements consist in applying an external magnetic field which causes lossless shielding currents to flow mostly along the perimeter of the sample. In the case of strong magnetic flux pinning, the model proposed in the 60's by C.P. Bean in infinite geometry [6] assumes that the density of the

screening currents is equal to the critical current density J_c. Therefore an appropriate mathematical treatment of magnetic measurements allows the critical current density J_c to be determined indirectly.

There are several methods for magnetic J_c measurements, which can be classified in AC or DC techniques [7]. The magnetic flux profile method, as proposed first by Campbell [8] and Rollins [9], is a convenient and straightforward AC measurement technique for determining J_c. It requires a primary coil generating an AC magnetic field and a secondary "pick-up" coil measuring the AC magnetic flux. Its advantage over other techniques is that it can probe volume properties of bulk superconducting samples of any size, in contrast to those relying on classical AC susceptometers and DC magnetometers which usually accommodate small samples (a few mm³), with some exceptions [10-13]. Basically, the flux profile technique involves applying an AC magnetic field of amplitude H_0, and recording the flux amplitude $\Phi(H_0)$ in the sample for several increasing values of H_0, as illustrated schematically in figure 1a. If the critical current density is assumed to be independent of H_0, the penetration depth p of magnetic flux inside the sample is directly related to the derivative $d\Phi(H_0)/dH_0$ [8,14]. The plot of H_0 vs. p is called *flux profile*, whose slope is proportional to the local critical current density of the sample. A flux profile measurement represents therefore a convenient way of indirectly probing the local critical current density variations in a high-temperature superconductor [15]. Moreover, in the case of granular superconducting ceramics, the flux profiles have been shown to exhibit a pronounced kink, as shown in figure 1b; the two slopes of the flux profile are related to the *inter-* and *intra-* granular critical current densities [14,16]. A careful examination of the flux profiles measured at several frequencies and magnetic field configurations allows also more fundamental physical parameters to be determined, such as the thermal activation energy of flux lines [17], or pinning lengthscales and flux line lattice constants [18,19]. It can also be used to assess the quality and homogeneity of the bulk material, e.g. in melt-textured YBCO [20] as well as in MgB_2 [21].

The extraction of the critical current density from the flux profile also depends on the sample geometry. Flux profile calculations which have been published in the literature concern only isotropic samples having either an infinite slab or infinite cylinder geometry, as sketched in figure 2a. The aim of the present work is to extend calculations of flux profiles in the case of *parallelipipedic* samples of rectangular cross-section $a \times b$ (figure 2b), which are relevant to bulk single domain superconductors and single crystals. In addition, we will investigate how the anisotropy of J_c and / or the shielding current lengthscales affect the measured signal. Finally, flux profile measurements carried out on bulk melt-processed $YBa_2Cu_3O_{7-\delta}$ samples will be presented, and the results will be compared to the theoretical predictions.

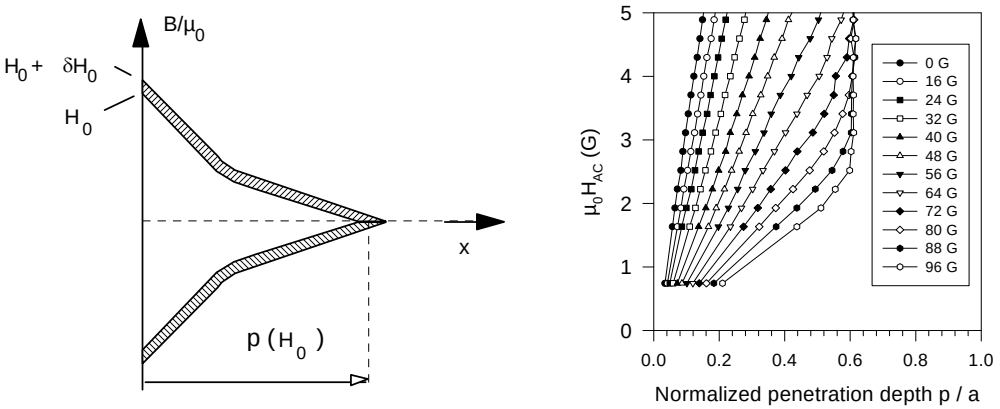

Figure 1. (a) Schematic representation of the magnetic flux density B at the edge of the sample as a function of distance x for two applied AC magnetic fields H_0 and $H_0 + \delta H_0$. (b) Flux profiles measured on a YBCO ceramic sample at 77K for different superimposed DC fields (see legend), showing clearly the appearance of a "kink" for the largest DC fields.

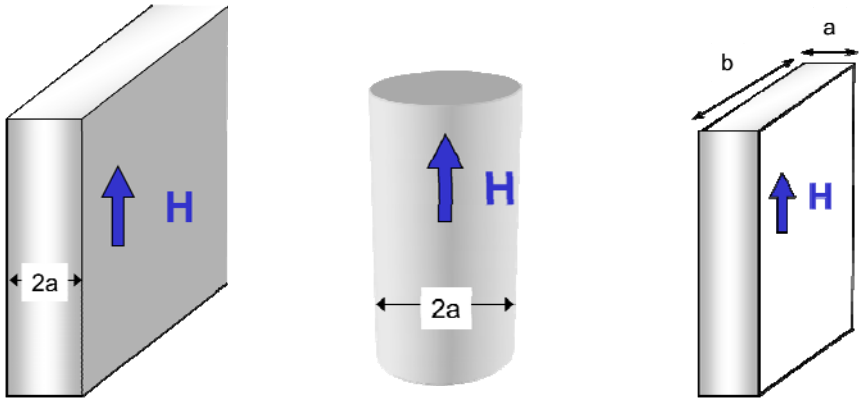

(a) (b)

Figure 2. (a) Two geometries for which analytical calculations of magnetic flux profiles are available in the literature (infinite slab and infinite cylinder). (b) Geometry investigated in the present work (infinite prism of rectangular cross-section).

2. Theory

2.1. General considerations

As recalled above, the key point of the Campbell method is that the derivative of the magnetic flux Φ with respect to the magnetic field amplitude H_0 gives access to the magnetic flux penetration depth $p(H_0)$. For a sample approximated either by an infinite slab of thickness $2a$ or by an infinite cylinder of diameter $2a$ (cf. figure 2a), the penetration depths are given respectively by [8,9,14]

$$p(H_0) = a\left(\frac{\frac{d\Phi}{dH_0}}{\frac{d\Phi_N}{dH_0}}\right) \quad \text{or} \quad p(H_0) = a\left[1-\sqrt{1-\left(\frac{\frac{d\Phi}{dH_0}}{\frac{d\Phi_N}{dH_0}}\right)}\right], \tag{1}$$

where Φ_N denotes the magnetic flux in the normal state (i.e. above the critical temperature T_c). The quantity $(d\Phi/dH_0) / (d\Phi_N /dH_0)$ is involved in both above formulas and represents a normalized flux-derivative which can be determined easily by two experiments (one in the superconducting state below T_c and one in the normal state above T_c) , it will be noted hereafter by the letter F, i.e.

$$F = \frac{\left(\frac{d\Phi}{dH_0}\right)}{\left(\frac{d\Phi_N}{dH_0}\right)}. \tag{2}$$

The purpose of the present section is to find the analytical expressions for F as a function of the sample parameters (J_c and geometry) in the case of a bulk sample with a rectangular cross-section ($b \geq a$). The sample is assumed to be infinite in the direction parallel to the magnetic field H; in order to keep a finite magnetic moment however, we will consider a layer of thickness z. In the following calculations, we also assume that J_c is independant of H_0.

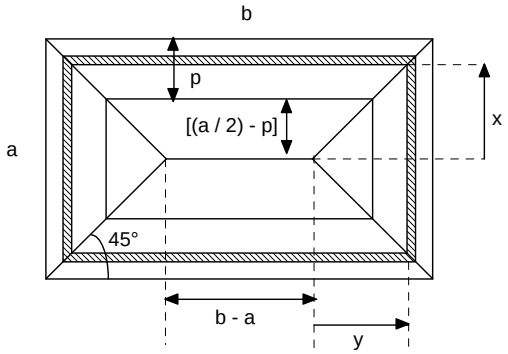

Figure 3. Cross-section of a rectangular the sample with dimensions *a* and *b* in the isotropic case. The supercurrents are assumed to flow along rectangular paths (shaded area). The solid interior lines show the field meeting lines when the sample is fully penetrated.

The principle of the flux profile determination involves calculating the magnetic moment *m* caused by rectangular shielding currents loops in the sample, as depicted in figure 3. Hence the magnetization *M* is obtained by dividing the magnetic moment *m* by the sample volume. By replacing $\Phi = ab\,\mu_0(H_0 + M)$ and $\Phi_N = ab\mu_0 H_0$ in Eq. (2) the normalized derivative *F* is given by

$$F = 1 + \frac{dM}{dH_0}. \tag{3}$$

2.2. Rectangular sample with isotropic critical current density $J_{cx} = J_{cy} = J_c$

Figure 3 shows a sketch of both sample geometry and current loops for an applied magnetic field of amplitude H_0. The current density is assumed to be the same for both directions, i.e. $J_{cx} = J_{cy} = J_c$. The penetration depth of magnetic flux, *p*, is equal to H_0 / J_c. The area delimited by the shaded current loop, situated at a distance *x* from the flux corner, is given by

$$A(x) = (2x)\left[2x + (b - a)\right]. \tag{4}$$

The total magnetic moment m is given by

$$\begin{aligned} m &= \int_{a/2-p}^{a/2} A\,di = \int_{a/2-p}^{a/2} A(x) J_c t\,dx \\ &= 2J_c zp\left[\frac{2p^2}{3} - \frac{p}{2}(a+b) + \frac{ab}{2}\right]. \end{aligned} \tag{5}$$

In the particular case $p = a/2$ (full penetration condition), the above formula becomes

$$m\left(p = \frac{a}{2}\right) = \frac{J_c t a^2}{4}\left(b - \frac{a}{3}\right), \tag{6}$$

in accordance with the results published some time ago by Gyorgy et al. [22]. The resulting global magnetization *M* is negative and equal to the magnetic moment divided by the sample volume, i.e.

$$M = -|M| = -\frac{m}{V} = -\frac{m}{abz} = -\frac{2J_c}{ab}\left[\frac{2}{3}p^3 - \frac{(a+b)}{2}p^2 + \frac{ab}{2}p\right]. \quad (7)$$

Finally, the normalized flux-derivative F is given by

$$F = 1 + \frac{dM}{dH_0} = 1 + \frac{1}{J_c}\left(\frac{dM}{dp}\right) = \frac{2(a+b)}{ab}p - \frac{4}{ab}p^2. \quad (8)$$

This equation is only valid when the magnetic flux penetration depth, $p = H_0 / J_c$, is smaller than the half of the smallest side of the rectangular cross-section (a/2), even at the highest applied AC magnetic field amplitude H_0. Such a condition is realistic in practice since bulk (RE)BCO large grain superconductors (where "RE" denotes a rare-earth ion) are characterized by large J_c values [5].

2.3. Rectangular sample with anisotropic critical current density $J_{cx} \neq J_{cy}$

When the current density is anisotropic, the cases ($J_{cx} \geq J_{cy}$) and ($J_{cx} \leq J_{cy}$) need to be examined separately. Figure 4 shows a sketch of current loops within a rectangular sample ($b \geq a$) for which the critical current density along the x-direction J_{cx} is larger than along the y-direction J_{cy}. The anisotropy ratio J_{cx} / J_{cy} is denoted by r (in the case of figure 4, one has $r \geq 1$). Taking into account the conservation of the total current flow and defining p_y as the penetration depth of magnetic flux along the y-direction, is equal to ($p_y = H_0 / J_{cy}$), the magnetic moment m is given by

$$m = \frac{2J_{cy}p_y za^2}{r}\left[\frac{2}{3}\left(\frac{p_y}{a}\right)^2 - \frac{1}{2}\left(\frac{p_y}{a}\right) + \frac{r}{2}\frac{b}{a}\left(1 - \frac{p_y}{a}\right)\right]. \quad (9)$$

Note that in the particular case $p_y = a/2$ (full penetration condition), the above formula becomes

$$m\left(p_y = \frac{a}{2}\right) = \frac{J_{cy}ta^2}{4}\left(b - \frac{a}{3r}\right), \quad (10)$$

in accordance with the calculations published in the literature [22]. The normalized flux-derivative F as defined by Eq. (2) is given by

$$F = \frac{2(a+br)}{abr}p_y - \frac{4}{abr}{p_y}^2. \quad (11)$$

The above calculations assumed that the critical current density along the x-direction J_{cx} was larger than along the y-direction J_{cy}, which led to an anisotropy ratio $r = J_{cx} / J_{cy}$ larger than unity. In the opposite case ($r \leq 1$), two different situations arise. If the ratio (a / 2r) is smaller than b/2, the current loops illustrated in Figure 2a are valid and the above calculations are still correct. If a / 2r is larger than b/2 - which arises when $a > br$ - the current loops are similar to those shown in figure 2b. The corresponding formulations for magnetic properties can be easily obtained through interchanging x and y axes. This procedure leads to

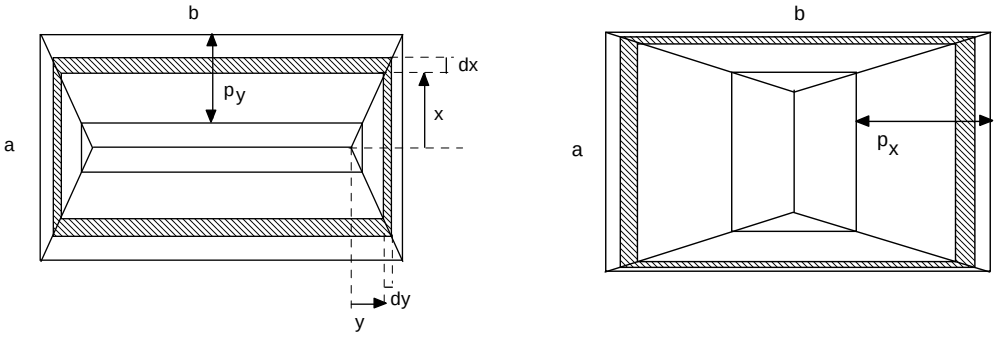

Figure 4. Supercurrent paths within a rectangular sample which exhibits a critical current density anisotropy, in the case $J_{cx} > J_{cy}$ (left) or $J_{cx} < J_{cy}$ (right).

$$m = 2J_{cx}p_x zrb^2\left[\frac{2}{3}\left(\frac{p_x}{b}\right)^2 - \frac{1}{2}\left(\frac{p_x}{b}\right) + \frac{1}{2r}\left(\frac{a}{b}\right)\left(1-\frac{p_x}{b}\right)\right]. \quad (12)$$

In the full-penetration limit $p_x = b/2$, the magnetic moment is given by

$$m = \frac{J_x tb^2}{4}\left(a - \frac{br}{3}\right). \quad (13)$$

Finally, the flux-derivative F is given by

$$F = \frac{2(a+br)}{ab}p_x - \frac{4r}{ab}{p_x}^2. \quad (14)$$

3. Discussion

3.1. The influence of the sample geometry

As can be seen in Eq. (8), (11) and (14), the normalized flux derivative F is a *parabolic* function of the penetration depth p, although J_c is assumed to be a constant. The non-linearity is thus a geometric effect which arises from the penetration of flux through *both* (orthogonal) faces of the sample. As a consequence, using a slab or cylinder approximation for a rectangular geometry always leads to the following errors : (i) an underestimation of J_c; the error being often in the range 10-20 % and (ii) a non-physical curvature of flux profiles.

3.2. The influence of lengthscale of shielding currents

The determination of J_c from the slope of the flux profiles assumes that shielding (critical) currents flow on a macroscopic lengthscale, fixed by the dimensions of the sample cross-section. Any defect in the microstructure (macro crack, grain boundary,...) may result in an alteration of this lengthscale, i.e. smaller shielding current loops. In the present section we want to investigate how a reduction of the lengthscale affects the flux profiles determined by the Campbell method. This has been done here for a superconducting sample with rectangular cross-section $a = s$, $b = 2s$, where s denotes a fixed and known length (e.g. s = 1mm). The magnetic moment m_1 generated by shielding currents in the sample shown in in the inset of figure 5a is given by

$$m_1 = m(s,2s) = 2J_c tp\left[\frac{2p^2}{3} - \frac{p}{2}(s+2s) + \frac{s(2s)}{2}\right]. \quad (15)$$

Suppose that a very weak link ($J_c \approx 0$) parallel to a divides the sample into two identical squared parts of side *s*; the lengthscale of shielding currents is now reduced, as shown in the inset of figure 5a The magnetic moment m_2 of this sample is given by

$$m_2 = 2m(s,s) = 4J_c tp\left[\frac{2p^2}{3} - \frac{p}{2}(s+s) + \frac{s^2}{2}\right] < m_1. \quad (16)$$

Similarly, a sample split into 4 identical parts is characterized by a magnetic moment m_4 given by

$$m_4 = 4m\left(\frac{s}{2},s\right) = 8J_c tp\left[\frac{2p^2}{3} - \frac{p}{2}\left(s+\frac{s}{2}\right) + \frac{s}{2}\left(\frac{s}{2}\right)\right] < m_2 < m_1. \quad (17)$$

Suppose now that the Campbell flux profile method is applied on each of the 3 above samples, and that the flux penetration depth is calculated from the measured flux derivatives *F* by inserting the *whole* sample dimensions, $a = s$ and $b = 2s$, in Eq. (15), (16), (17). This procedure is equivalent to ignoring the weak links and assuming that shielding currents flow on a scale on the order of the sample size. The results are shown in figure 5a. The presence of one or two weak links located in the middle of the sample is clearly seen to affect the *slope* of the flux profiles, whatever the formula used for its determination. Such a situation is quite different from the case of granular samples for which a weak-link network results in a pronounced *kink* in the flux profile [14,16]. In ceramics, the kink is visible because of a non-negligible proportion of weak links in the sample. In the case of isolated weak links, the intergrain volume is small and all flux profiles are linear. As a consequence, the above simulation shows that isolated weak links may strongly affect the flux profiles determined by the Campbell method. However their effects cannot be distinguished from an intrinsically small critical current density.

3.3. Anisotropy effects

In this section we want to examine the effect of an anisotropic J_c on the problem of shielding current lengthscales discussed in Sect. 3.2 above. As an example, we compare the *slope* of the flux derivative, dF / dH_0, for a "single grain" (SG) rectangular sample with dimensions $a \le b$, and for a "double grain" (DG) sample consisting in a juxtaposition of two rectangular samples of dimensions $a \le (b/2)$. The magnetic moment m_{SG} of the SG sample and the corresponding normalized flux derivative, F_{SG}, are given by Eq. (9) and (11). From them we can calculate the initial slope (denoted S_{SG}) of the magnetic flux profile (H_0,F_{SG}) plot; this slope is given by

$$S_{SG} = \left\{\frac{d}{dH_0}F_{SG}\right\}_{H_0=0} = \frac{1}{J_{cy}}\left(\frac{2}{abr}\right)(a+br). \quad (18)$$

A similar procedure for the double grain (DG) sample, yields an initial slope (S_{DG}) given by

$$S_{DG} = \left\{\frac{d}{dH_0}F_{DG}\right\}_{H_0=0} = \frac{1}{J_{cy}}\left(\frac{2}{abr}\right)(2a+br). \quad (19)$$

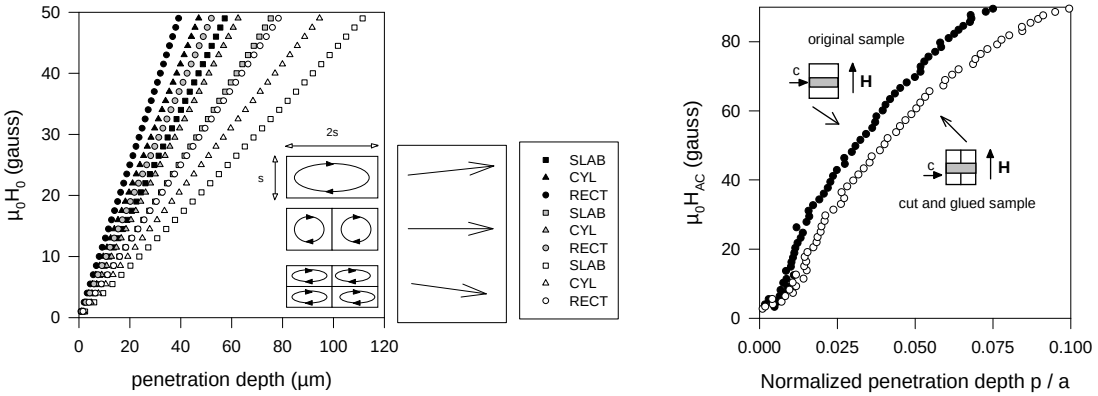

Figure 5. (a) Comparison of the calculated flux profiles for the different "lengthscaled" samples 1, 2 and 4 schematically illustrated in the inset. The critical current density J_c is assumed to be equal to 10^4 A/cm². The flux profiles are calculated by approximating the rectangular cross-section by either a slab (squares) of thickness s or a cylinder (triangles) of equivalent radius $R = (2/\pi)^{1/2}\, s$. The circles refer to the flux profiles calculated using the formulas of the present paper, with no assumption on the cross-section. (b) Comparison of the flux profiles measured for two superconducting bulk YBCO samples, (i) the original single grain (SG) sample (black symbols) and (ii) a split double grain (DG) sample. The measurement is carried out at $T = 77$ K. The applied DC magnetic induction is 1500 gauss (0.15 T).

From Eq. (18) and (19), the ratio of the slopes of the magnetic flux profiles in the two cases, S_{DG} / S_{SG}, is given by

$$\frac{S_{DG}}{S_{SG}} = \frac{2a + br}{a + br} \quad (\geq 1) \tag{20}$$

Several observations can be drawn from the above equation. First, the slope $S = \mathrm{d}F / \mathrm{d}H_0$, which is inversely proportional to the "apparent" critical current density J_c, is clearly higher for the split sample than for the original one. However, in the limit case $r >> 1$, Eq. (20) shows that both slopes are the same. Indeed, in such a case, the equivalent "thickness" of current flow parallel to a, is negligible with respect to the sample dimensions, and currents in the vicinity of the cutting plane cancel out each other. This theoretical result will be compared to the experimental result in the next section.

4. Experiment

Flux profile measurements on a superconducting $YBa_2Cu_3O_{7-\delta}$ single domain are carried out in order to illustrate how the theoretical formulas developed above can be applied in practice. The single domain material is synthesised by a method described elsewhere [23,24]. The samples are characterized by the following superconducting parameters : critical current density $J_c = 10^4$ A/cm² and $T_c = 89$ K. Measurements of the critical current density for both directions gives an anisotropy ratio (J_c^{ab} / J_c^{c}) close to 3 at low magnetic inductions (< 0.5 T) [24,25].

Since the theoretical results clearly show (cf. Eq. (20)) that flux profile measurements are sensitive to the lengthscale over which shielding currents flow, the question we want to address is whether the shielding current loops when the magnetic field is applied parallel to the *ab* planes (and hence

shielding currents do have a component parallel to the *c*-axis) are *macroscopic*, i.e. flow along the perimeter of the sample, or *microscopic*, i.e. flow along small circular loops because of the numerous microcracks and platelet boundaries in the single domain. To answer this question, magnetic flux profiles are first measured on a single grain sample with the applied field parallel to *ab* ("original" sample). Then the specimen is cleaved along the *ab* planes, both identical parts are repositioned side by side, glued with insulating GE varnish, and the same measurement is repeated ("cut and glued" sample). The sample geometries and results are summarized in figure 5b. When comparing both curves, it turns out that for a given magnetic field value, the AC penetration depth is higher in the case of the cleaved sample than for the original large specimen. The average slopes are found to differ by 12 %. From the results worked out above (Eq. 20), the ratio of slopes measured for single grain (SG) and double grain (DG) can be calculated analytically, knowing the dimensions of the original specimen cross section ($b \geq a$), and the anisotropy ratio r ($= J_c^{ab} / J_c^{c}$). In the present case, one has $b = 2a$ and $r \approx 3$. By assuming macroscopic shielding current loops, the theoretical ratio is thus given by $S_{DG} / S_{SG} = 1.14$. This result is in fairly good agreement with the measured data (1.12). In contrast, if the current loops were microscopic, i.e. much smaller than the sample dimensions, the flux profiles would not be influenced by the cutting / rejoining process. Consequently, the measurement result gives experimental evidence that shielding currents globally flow over a lengthscale comparable to the sample size, despite the presence of cracks and platelet boundaries. As discussed in ref. [24], the examination of $M(H)$ loops on the same sample leads the same conclusion, but the sensitivity of the experiment is much more pronounced in the present case.

From this result we can conclude that the magnetic flux profiles are not only helpful in bringing out current density inhomogeneities but also in examining the influence of shielding currents lengthscales in bulk, large grain superconducting samples.

5. Conclusion

In this paper we developed analytical expressions relevant to the magnetic flux profile methods. Generally speaking, these methods consist in applying an external AC magnetic field and recording the magnetic flux Φ threading the sample cross-section, in order to deduce the penetration depth p as a function of the AC field amplitude H_0. If the AC field is superimposed to a bias DC field, the critical current density J_c may be assumed to be field-independent. In such a case, the slope of the flux profile gives the local critical current density. In the present work, flux profiles were calculated for samples of rectangular cross-section characterized by a field-independent but anisotropic critical current density. Such a model is quite appropriate for a crystal-like superconducting sample, e.g. a single crystal or a bulk, large grain YBCO superconductor. The effects resulting from approximating the parallelipipedic geometry by either a cylinder or a slab geometry were discussed. It was also shown that a few isolated weak links in the material affect the *slope* of the flux profile. Such a situation differs from a ceramic containing a weak link network, which results in a *kink* in the flux profile. Finally, we showed how the slope of flux profiles is influenced by the lengthscale of shielding currents. In the case of bulk melt-textured sample with applied field parallel to *ab* plane, the theoretical results were found to agree nicely with experiments.

Acknowledgements

We thank the University of Liège (ULg) and the Ministry of Higher Education of *Communauté Française de Belgique* for a research grant *Action de Recherches Concertées* (ARC 11/16-03). We thank Prof. M. Ausloos, A.M. Campbell, D.A. Cardwell for many fruitful discussions. The help of W. Lo and R. Cloots for supplying the superconducting sample is also acknowledged. This work is part of a collaboration programme financed by Wallonie Bruxelles International (WBI, Belgium) and the Bulgarian Academy of Sciences (BAS, Bulgaria).

References

[1] Masson P J, Breschi M, Tixador P and Luongo C A 2007 *IEEE Trans. Appl. Supercond.* **17** 1533
[2] Ma G T, Lin Q X, Wang J S, Wang S Y, Deng Z G, Lu Y Y, Liu M X and Zheng J 2008 *Supercond. Sci. Technol.* **21** 065020
[3] Hsu C H, Yan Y, Hadeler O, Vertruyen B, Granados X and Coombs T A 2012 *IEEE Trans. Appl. Supercond.* **22** 7800404
[4] Cardwell D A *et al.* 2005 *Supercond. Sci. Technol.* **18** S173
[5] Devendra Kumar N, Rajasekharan T, Muraleedharan K, Banerjee A and Seshubai V 2010 *Supercond. Sci. Technol.* **23** 105020
[6] Bean C P 1964 *Rev. Mod. Phys.* **1** 31
[7] Frischherz M C, Sauerzopf F M, Weber H W, Murakami M and Emel'chenko G A 1995 *Supercond. Sci. Technol.* **8** 485
[8] Campbell A M 1969 *J. Phys. C* **2** 1492
[9] Rollins R W, Küpfer H and Gey W 1974 *J. Appl. Phys.* **45** 5392
[10] Vanderbemden P 1998 *Cryogenics* **38** 839
[11] Laurent P, Fagnard J F, Vanderheyden B, Hari Babu N, Cardwell D A, Ausloos M and Vanderbemden P 2008 *Meas. Sci. Technol.* **19** 085705
[12] Chen D X 2004 *Meas. Sci. Technol.* **15** 1195
[13] Trojanowski S and Ciszek M 2007 *Prz. Elektrotech.* **83** 26
[14] Küpfer H et al. 1988 *Cryogenics* **28** 650
[15] Eckert D and Handstein A 1976 *Phys. Status Solidi A* **37** 171
[16] Dang A, Godelaine P A, Vanderbemden P, Cloots R and Ausloos M 1995 *J. Appl. Phys.* **77** 3560
[17] Vanderbemden P, Destombes C, Cloots R and Ausloos M 1998 *Supercond. Sci. Technol.* **11** 94
[18] Otabe E S, Ohtani N, Matsushita T, Ishikawa Y and Yoshizawa S 1994 *Jpn. J. Appl. Phys.* 33 996
[19] Matsushita T, Otabe E S and Ni B 1991 *Physica C* **182** 95
[20] Hari Babu N, Rajasekharan T and Seshu Bai V 2000 *Physica C* **330** 203
[21] Ni B, Morita Y, Liu Z, Liu C, Himeki K, Otabe E S, Kiuchi M and Matsushita T 2009 *IEEE Trans. Appl. Supercond.* **19** 3529
[22] Gyorgy E M, van Dover R B, Jackson K A, Schneemeyer L F and Waszczak J V 1989 *Appl. Phys. Lett.* **55** 283
[23] Lo W, Dewhurst C D, Cardwell D A, Vanderbemden P, Doyle R A and Astill D M 1996 *Appl. Supercond.* **4** 507
[24] Vanderbemden P, Bradley A D, Doyle R A, Lo W, Astill D M, Cardwell D A and Campbell A M 1998 *Physica C* **302** 257
[25] Vanderbemden P, Cloots R, Ausloos M, Doyle R A, Bradley A D, Lo W, Cardwell D A and Campbell A M 1999 *IEEE Trans. Appl. Supercond.* **9** 2308